

# Application Note

## High content label-free phenotypic screening of living cells

NANOLIVE 

This Application Note will cover how the 3D Cell Explorer 96focus performs high content label-free phenotypic screening and will show how this state-of-the-art technology can be used for in vitro preclinical toxicology and de-risking studies to increase translational relevance. Unlike traditional endpoint assays, live cell imaging captures kinetic data alongside high-resolution images, providing greater understanding of therapeutic mechanism of action, and cellular responses.

The 3D Cell Explorer 96focus imaging platform captures images from a 96-well plate at a high subcellular (200 nm) resolution label-free. Our AI-powered digital assays take this visual output and use machine learning to translate it into easy-to-understand, useful metrics to detect and quantify phenotypic changes including cytotoxicity, cell growth, and metabolic processes label-free with high precision.



Streamlined, automated workflows: save time and money



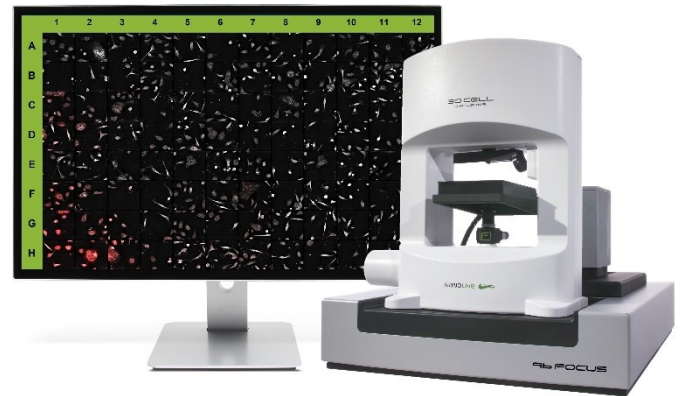
Unbiased and biologically relevant long-term monitoring of cells label-free



Increase predictive value of in vitro assays with high content, multiplexed, reliable live cell data

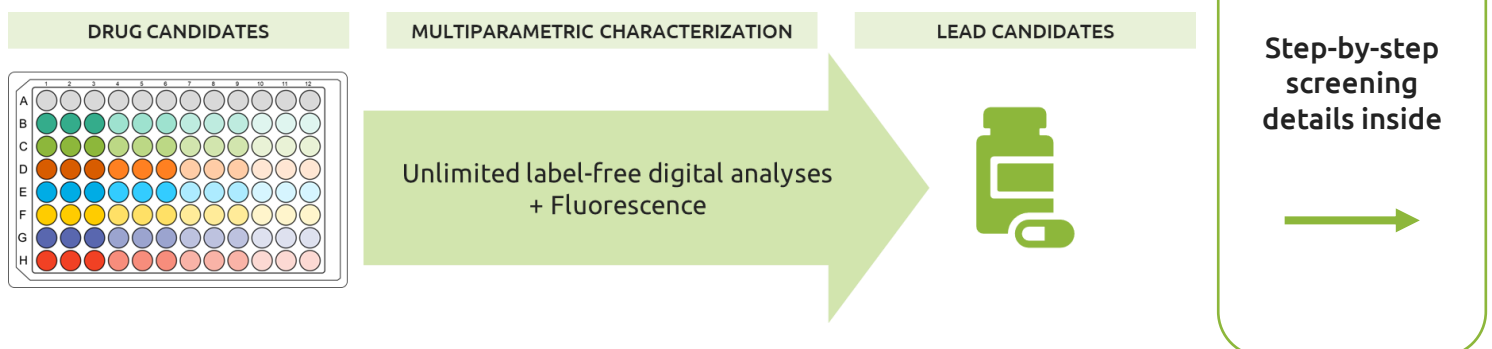


Accelerate drug discovery with fully integrated cutting-edge digital analytical solutions



## Use case: High content phenotypic screening

To increase confidence in lead candidates, Nanolive imaging platforms automatically measure and analyse cellular responses. The quantitative and qualitative data produced give a deeper understanding of the therapeutic mode of action, for more biologically relevant conclusions that can help to de-risk the following in vivo stage of drug development. This use case demonstrates how the 3D Cell Explorer 96focus can be used to run multiparametric screenings from a unique 96-well plate experiment.



# High content screen

## Part 1. Cytotoxicity screen with the LIVE Cell Death Assay



To increase confidence in lead candidates, Nanolive imaging platforms automatically measure and analyse cellular responses. The quantitative and qualitative data produced give a deeper understanding of the therapeutic mode of action, for more biologically relevant conclusions that can help to de-risk the following in vivo stage of drug development. This use case demonstrates how the 3D Cell Explorer 96focus can be used to screen drugs for multiple characteristics in parallel, in a 96-well plate.

## Experimental approach

The goal of this high content screen was to select a lead candidate drug to target a metabolic disorder. The desirable candidate should be non-cytotoxic, thus it should not cause an increase in reactive oxygen species (ROS), which could be a sign of damage to the cells.

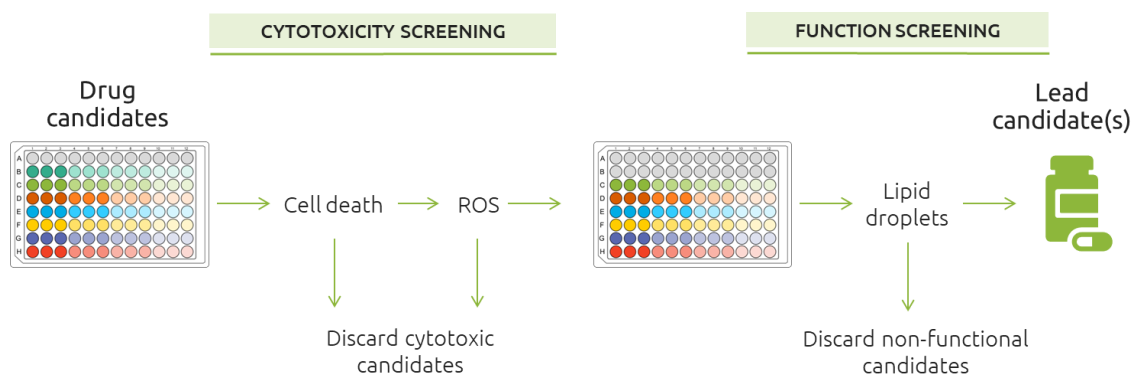


## Plate layout

One 96-well plate was used to investigate 6 drugs at 4 concentrations each, plus controls, (3 replicates). Pre-adipocytes were plated at equal confluency in each well. The top two rows contained positive and negative controls, and the other 6 rows contained one drug each at decreasing concentration left to right (3 replicates of each). The 96-well plate capacity allowed each of these conditions to be tested in parallel in the same experiment.

One refractive index image, and one fluorescent image was taken from each well, every hour.

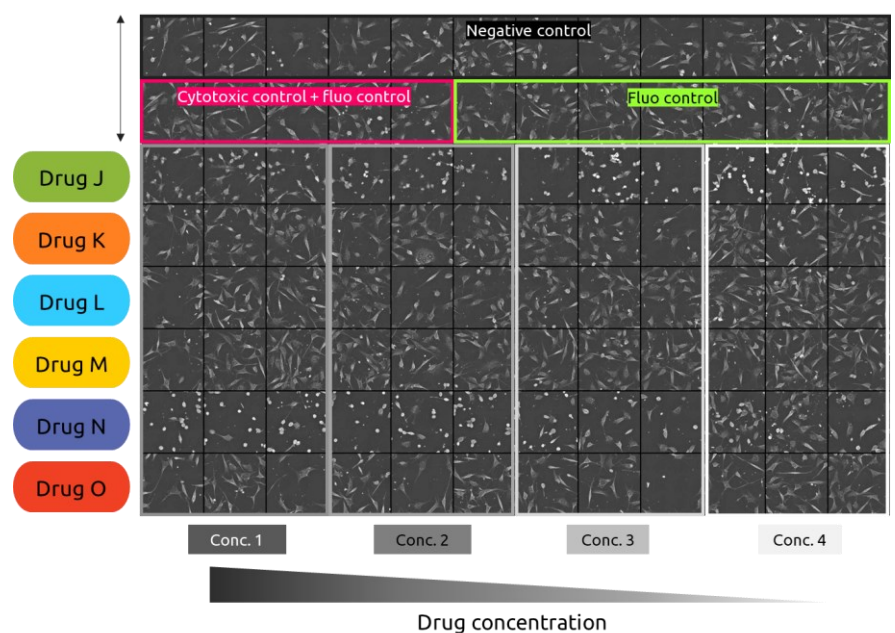


Plate overview with refractive index imaging at the first timepoint.

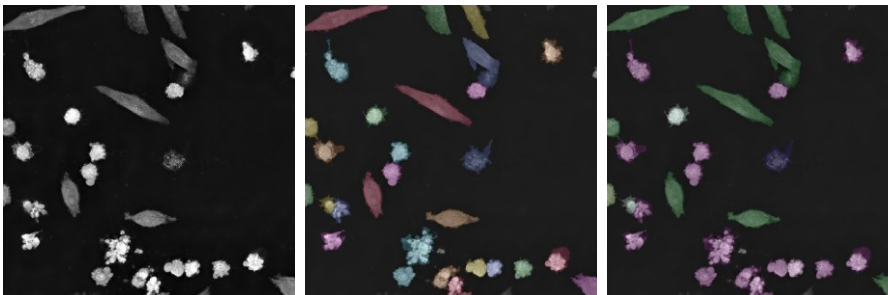
# High content screen

## Part 1. Cytotoxicity screen with the LIVE Cell Death Assay



The LIVE Cell Death Assay (LCDA) can be used in drug discovery for automatic quantification of cell health and death, detecting drug resistance, and monitoring cell recovery. The LCDA distinguishes between living, apoptotic, and necrotic cells completely label-free, and the captured images provide insights into drug mechanism of action<sup>1,2</sup>.

HeLa



Illustrative image (not part of the experiment) of HeLa cells imaged by refractive index (left), segmented (center), and classified as living (green), apoptotic (pink), or necrotic (dark blue) by the LCDA (right).

## Results

The mean cell death fraction was used to quantify cell death over time (Fig. 1). Drugs, J, N, and O caused a rapid onset of cell death, in all concentrations tested (Drug J shown in Fig. 1A). These drugs were cytotoxic at all concentrations, and therefore all concentrations of these drugs were excluded from the screening. Drug K caused cell death at the two highest concentrations tested, which were excluded from the next stage of screening. After 24 hours there was no significant difference in cell death between the controls (in fluorescent green and black) and cells treated with Drugs L or M at any concentration (Fig. 1B), or the two lowest concentrations of Drug K.

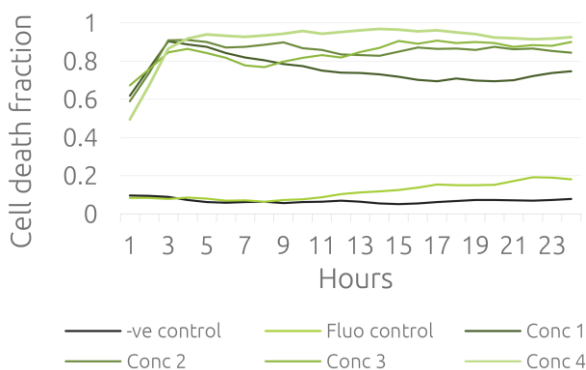


Figure 1A. Example of a cytotoxic drug candidate (Drug J) that caused rapid cell death within the first 3 hours of imaging. N=3

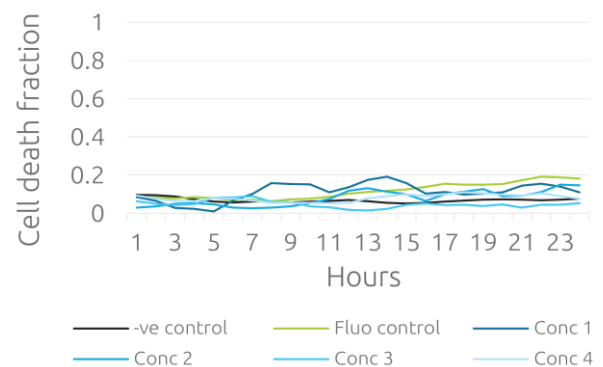
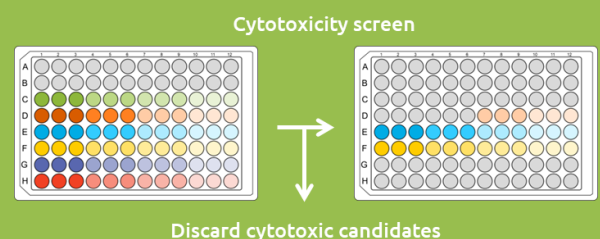


Figure 1B. Example of a non-cytotoxic drug candidate (Drug L). No significant cell death was observed in comparison to controls (black and green lines). N=3

This cytotoxicity screen allowed 14 out of 24 conditions to be excluded from further screening. Drugs L and M, and Drug K (2 lowest concentrations) were passed to the next screening step.



# High content screen

## Part 2. ROS screen with fluorescent probe



Drug treatments can cause mitochondrial dysfunction, leading to morphological changes, production of ROS and oxidative stress. Monitoring mitochondrial response is of particular interest in this screen, due to its link to metabolic dysregulation and disorders such as cardiovascular disease, type 2 diabetes, and obesity<sup>3</sup>.

Nanolive imaging is an effective method used to study mitochondrial perturbation and dynamics in real-time<sup>4-6</sup>. Here, we chose to detect reactive oxygen species (ROS) using the fluorescent probe CellROX™ (Thermofisher)<sup>7</sup>. Cells were exposed to Cy5 fluorescence excitation for 300ms/cycle at 10% intensity.

## Results

The full plate capture layout made it easy to compare fluorescence in different samples. During the capture, fluorescence was visible in all concentrations tested of Drug K, but not Drug L or Drug M. Therefore Drug K provoked the production of ROS at all concentrations tested, and was excluded from the next stage of screening.

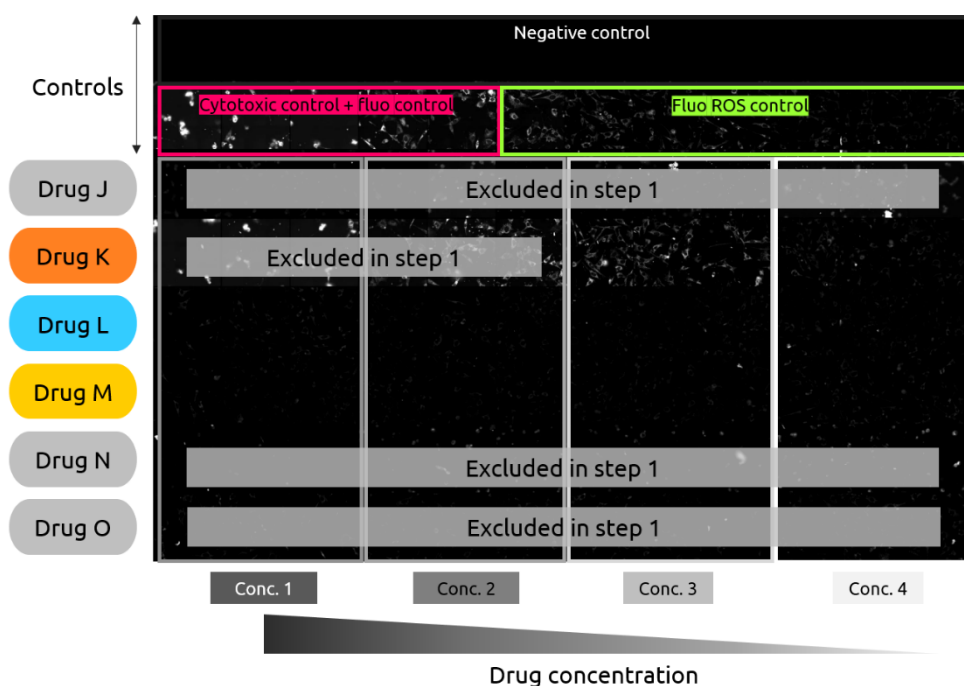
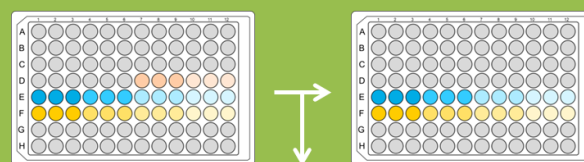


Plate layout showing fluorescence signal. Drugs and drug concentrations that were already excluded have been greyed out.

This step enabled detection of oxidative stress caused by drug treatments at concentrations that were not cytotoxic, adding greater sensitivity to our screening.



Discard candidates causing ROS

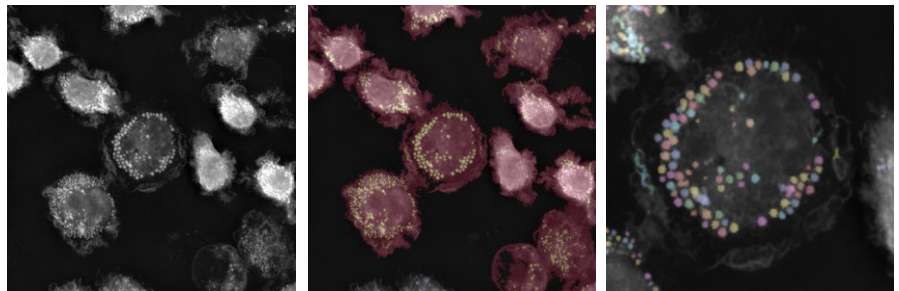
# High content screen

## Part 3. Metabolic screen with the Smart Lipid Droplet Assay



Lipid droplets are dense lipid stores in the cytoplasm, that play a role in metabolic regulation. They are translucent and cannot be detected using traditional light microscopy without using dyes. However, they have a high refractive index, so can be detected label-free using Nanolive imaging<sup>8,9</sup>. The Smart Lipid Droplet Assay segments lipid droplets and cell boundaries automatically to quantify changes in lipid droplets over time.

Quantifying the change in intracellular lipid droplets was important in this screen because we were looking for a drug that can be repurposed to treat metabolic disorders. An increase in lipid droplet accumulation may be desirable, for example for the treatment of lipodystrophies<sup>10</sup>, whereas for treating other diseases, a decrease, or maintenance of lipid droplet levels may be required. Nanolive's screening can be adapted to fit either need.



Illustrative image (not part of the experiment) of macrophage foam cells imaged by refractive index (left), cells as segmented by the SLDA (center), lipid droplets segmented by the SLDA (right).

## Results

Two drugs remained at this screening stage; Drug L and Drug M. The Smart Lipid Droplet Assay metric, Mean lipid droplet dry mass per cell over time was used to monitor changes in lipid accumulation inside cells. Drug L did not induce a change in mean lipid droplet dry mass per cell over time (Fig. 2A), but Drug M caused an increase in mean lipid droplet dry mass (Fig. 2B), indicating an increase in lipid accumulation inside cells.

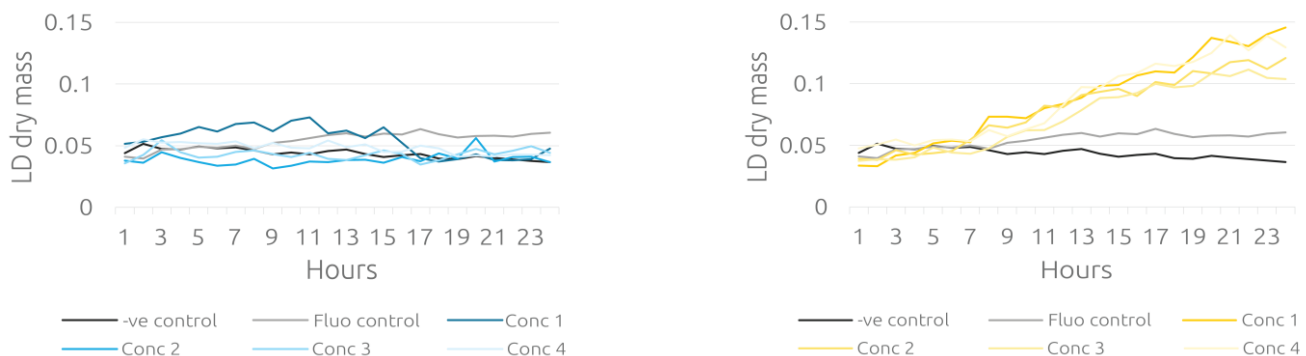
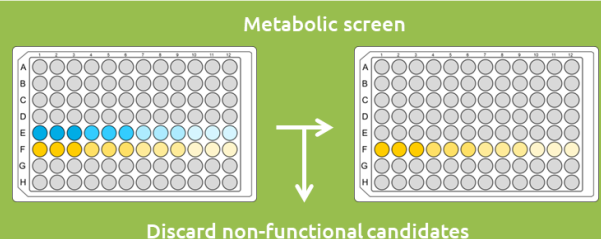


Figure 2. Mean lipid droplet dry mass per cell (pg) did not increase over time in cells treated with Drug L (A), but did increase in cells treated with Drug M (B). N=3

This step identified Drug M had a desirable mode of action, so it was selected as the lead candidate



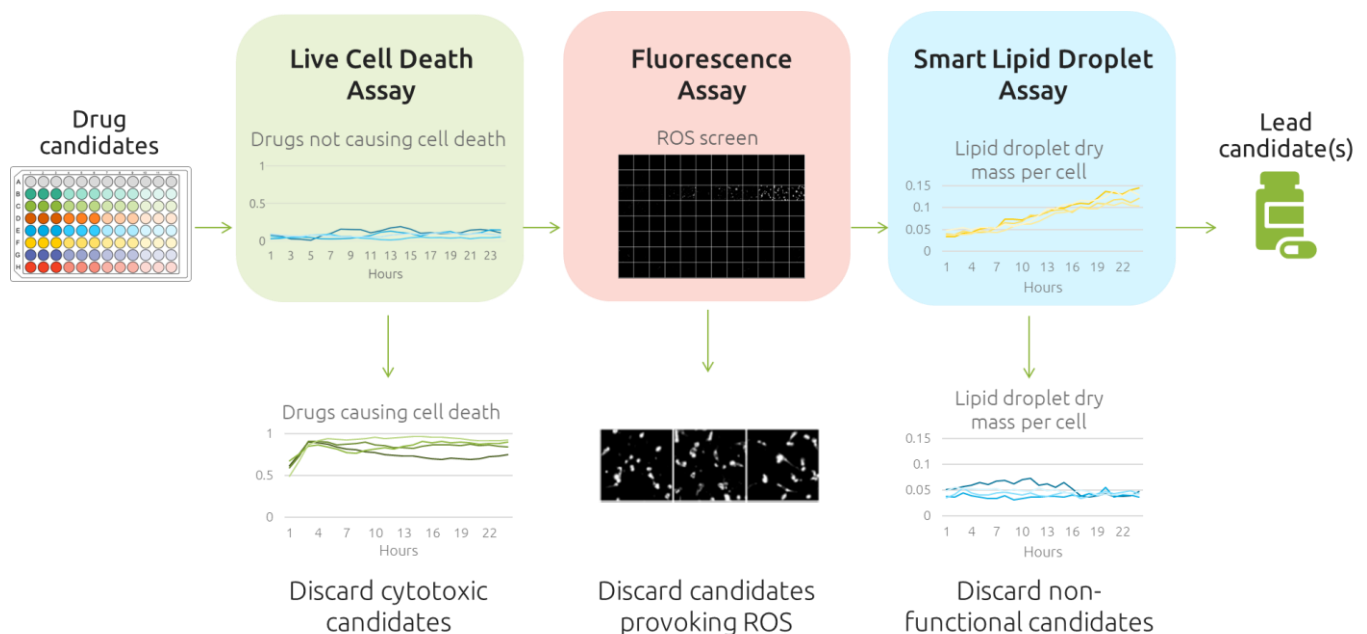
# High content screen Summary

NANOLIVE 

## Conclusion

In this example, 3 analyses were run on 6 drugs at 4 concentrations each, to measure cell death, presence of reactive oxygen species, and lipid droplet dry mass. Drugs were filtered out at each stage according to our parameters as illustrated in this overview schematic.

This functional screen allowed us to select the drug with the best chance of success in vivo according to our parameters: a drug that was non-cytotoxic, did not induce reactive oxygen species, and which altered cellular metabolism, as assessed by a change in lipid droplets. The analyses were completed retrospectively on imaging data gathered by the 3D Cell Explorer 96focus in a single run.



## Further steps

- Our digital assays can be used in any combination to look at different processes such as morphological changes, the type of cell death, and immune cell interactions, along with up to 4 fluorescence markers.
- All digital assays can be used retroactively to analyse and re-analyse data at a time convenient to you.
- Our 96-well plates are industry-standard and are compatible for use with other devices, for seamless transition to complementary downstream analysis methods, or continued cell culture.

## Benefits of a high content screen

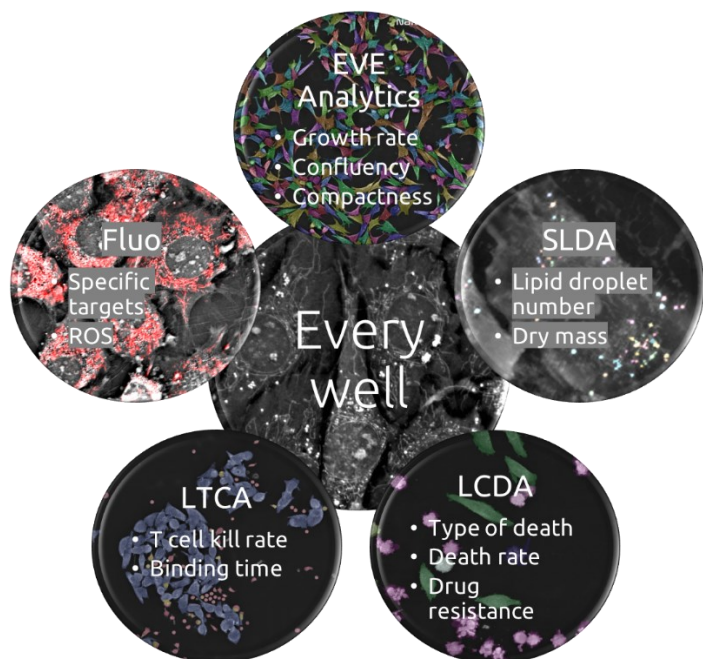
- ✓ Capture rich, multiplexed data
- ✓ Automatic analysis using machine learning
- ✓ Gain understanding of therapy effects and mechanism of action
- ✓ Better understanding at the in vitro stage

# Application Note

## High content label-free phenotypic screening of living cells

NANOLIVE 

## High content imaging, for multiplexed experiments



Gather data on each cell in every frame;

- EVE Analytics provides general metrics such as the growth rate, confluency, and compactness of cells over time
- The Smart Lipid Droplet Assay (SLDA) measures lipid droplet dry mass, size and number
- The LIVE Cell Death Assay (LCDA) monitors cell health and distinguishes between living, apoptotic, and necrotic cells
- The LIVE T cell assay (LTCA) monitors effector and target cell interactions and killing in coculture

The 3D Cell Explorer 96focus also comes with a 4-channel epifluorescence module, allowing you to further multiplex your acquisitions and look at specific targets of interest

## Use of Nanolive imaging in drug discovery

**Dr. John Ferbas**  
Director of Department of Medical Sciences,  
Amgen, USA

*On the SLDA: "Nanolive has developed a 'one-click assay' with no staining or centrifugation required, just a high-quality cell culture plus or minus the treatments of interest. This will allow us to learn orders of magnitude more about cell biology with less effort, less cost and greatly reduced infrastructure requirements relative to our legacy approaches."*

**Urs Lüthi**  
Associate Director and Deputy Head HTS,  
Idorsia Pharmaceuticals, Switzerland

*"Your data, with its dramatic resolution, provide a prime opportunity to measure the effect that a compound has on the morphology, pattern, and granularity of a cell, which we can use to predict the bioactivity of a compound. If we can identify compound-specific phenotypes, then we can screen other compounds for this phenotypic response and hypothesize that they function via a similar mechanism-of-action."*

For the latest peer-reviewed publications using Nanolive technology, visit our [website](#).

# Application Note

## High content label-free phenotypic screening of living cells

NANOLIVE 

## References

- (1) Mishima, E.; Ito, J.; Wu, Z.; Nakamura, T.; Wahida, A.; Doll, S.; Tonnus, W.; Nepachalovich, P.; Eggenhofer, E.; Aldrovandi, M.; Henkelmann, B.; Yamada, K.; Wanninger, J.; Zilka, O.; Sato, E.; Feederle, R.; Hass, D.; Maida, A.; Mourão, A. S. D.; Linkermann, A.; Geissler, E. K.; Nakagawa, K.; Abe, T.; Fedorova, M.; Proneth, B.; Pratt, D. A.; Conrad, M. A Non-Canonical Vitamin K Cycle Is a Potent Ferroptosis Suppressor. *Nature* **2022**, *608* (7924), 778–783. <https://doi.org/10.1038/s41586-022-05022-3>
- (2) Zan, R.; Wang, H.; Cai, W.; Ni, J.; Luthringer-Feyerabend, B. J. C.; Wang, W.; Peng, H.; Ji, W.; Yan, J.; Xia, J.; Song, Y.; Zhang, X. Controlled Release of Hydrogen by Implantation of Magnesium Induces P53-Mediated Tumor Cells Apoptosis. *Bioactive Materials* **2022**, *9*, 385–396. <https://doi.org/10.1016/j.bioactmat.2021.07.026>
- (3) Bhatti, J. S.; Bhatti, G. K.; Reddy, P. H. Mitochondrial Dysfunction and Oxidative Stress in Metabolic Disorders — A Step towards Mitochondria Based Therapeutic Strategies. *Biochimica et Biophysica Acta (BBA) - Molecular Basis of Disease* **2017**, *1863* (5), 1066–1077. <https://doi.org/10.1016/j.bbadis.2016.11.010>
- (4) Algieri, C.; Bernardini, C.; Marchi, S.; Forte, M.; Tallarida, M. A.; Bianchi, F.; La Mantia, D.; Algieri, V.; Stanzione, R.; Cotugno, M.; Costanzo, P.; Trombetti, F.; Maiuolo, L.; Forni, M.; De Nino, A.; Di Nonno, F.; Sciarretta, S.; Volpe, M.; Rubattu, S.; Nesci, S. 1,5-Disubstituted-1,2,3-Triazoles Counteract Mitochondrial Dysfunction Acting on F1FO-ATPase in Models of Cardiovascular Diseases. *Pharmacological Research* **2023**, *187*, 106561. <https://doi.org/10.1016/j.phrs.2022.106561>
- (5) Suh, J.; Kim, N.-K.; Shim, W.; Lee, S.-H.; Kim, H.-J.; Moon, E.; Sesaki, H.; Jang, J. H.; Kim, J.-E.; Lee, Y.-S. Mitochondrial Fragmentation and Donut Formation Enhance Mitochondrial Secretion to Promote Osteogenesis. *Cell Metabolism* **2023**, *35* (2), 345–360.e7. <https://doi.org/10.1016/j.cmet.2023.01.003>
- (6) Zapór, L.; Chojnacka-Puchta, L.; Sawicka, D.; Miranowicz-Dzierżawska, K.; Skowroń, J. Cytotoxic and Pro-Inflammatory Effects of Molybdenum and Tungsten Disulphide on Human Bronchial Cells. *Nanotechnology Reviews* **2022**, *11* (1), 1263–1272. <https://doi.org/10.1515/ntrev-2022-0073>
- (7) CellROX™. <https://www.thermofisher.com/order/catalog/product/C10422>
- (8) Larrazabal, C.; López-Osorio, S.; Velásquez, Z. D.; Hermosilla, C.; Taubert, A.; Silva, L. M. R. Thiosemicarbazone Copper Chelator BLT-1 Blocks Apicomplexan Parasite Replication by Selective Inhibition of Scavenger Receptor B Type 1 (SR-B1). *Microorganisms* **2021**, *9* (11), 2372. <https://doi.org/10.3390/microorganisms9112372>
- (9) Sandoz, P. A.; Tremblay, C.; Goot, F. G. van der; Frechin, M. Image-Based Analysis of Living Mammalian Cells Using Label-Free 3D Refractive Index Maps Reveals New Organelle Dynamics and Dry Mass Flux. *PLOS Biology* **2019**, *17* (12), e3000553. <https://doi.org/10.1371/journal.pbio.3000553>
- (10) Garg, A. Lipodystrophies: Genetic and Acquired Body Fat Disorders. *The Journal of Clinical Endocrinology & Metabolism* **2011**, *96* (11), 3313–3325. <https://doi.org/10.1210/jc.2011-1159>

## Contact us

Would you like to enquire about our products? Please contact us directly via phone, email or webform.

**Phone:** +41 21 353 0600

**Email:** [lookinginsidelife@nanolive.ch](mailto:lookinginsidelife@nanolive.ch)

**Webform:** <https://www.nanolive.ch/enquire-now/>